



# New Cyanide-Free Alkaline Electrolyte for the Electrodeposition of Cu-Zn Alloys Using Glutamate as Complexing Agent

P. Pary,<sup>1,2,z</sup> L. N. Bengoa,<sup>1,2</sup> P. R. Seré,<sup>1</sup> and W. A. Egli<sup>1</sup>

<sup>1</sup>Center for Paints and Coatings Development (CICBA-CONICET-UNLP), La Plata B1900AYB, Argentina

<sup>2</sup>Engineering School, National University of La Plata, La Plata B1900AYB, Argentina

Glutamate is a potential replacement of cyanide in alkaline electrolytes due to its capability to form complexes with bivalent metal ions. Since promising results were achieved with copper and zinc plating baths, and the use of cyanide implies environmental and safety disadvantages, it was decided to study the possibility of codepositing these two metals using sodium glutamate as complexing agent. Electrochemical processes involved in electrodeposition of copper and zinc individually as well as in solutions containing both metal ions were studied utilising cyclic voltammetry. Cu-Zn deposits obtained at different current densities from solutions of different composition were characterized by SEM and EDS. It was concluded that the system has a normal behavior, according to Brenner's classification, since the more noble metal is deposited preferentially. The plating bath containing 30% molar of Cu<sup>2+</sup> was selected to continue the studies of the system.

© 2019 The Electrochemical Society. [DOI: 10.1149/2.0691902jes]

Manuscript submitted November 5, 2018; revised manuscript received December 12, 2018. Published January 19, 2019.

Alkaline electrolytes are used to produce thin coatings (strike coatings) on substrates which suffer corrosion in acid media. These metallic deposits serve as a protective layer for subsequent processes such as acid copper, nickel and chromium plating. Complexing agents are needed in these electrolytes in order to maintain the metallic ion in solution and avoid the formation and precipitation of oxides and hydroxides. The most common alkaline electrolytes used to obtain metallic deposits of copper, zinc and their alloys contain cyanide as the main complexing agent in their formulation.<sup>1-3</sup> Although deposits resulting from the use of these electrolytes are of good quality, their high toxicity and extremely negative impact on the environment during waste disposal<sup>4</sup> have become a strong driving force for their replacement with less toxic baths. During the last decades many electrolytes have been proposed for cyanide replacement: being the most important formulations based on pyrophosphate,<sup>5-8</sup> glycerol,<sup>5</sup> nitrilotriacetate,<sup>9</sup> glycine<sup>10,11</sup> and copper and zinc sulfates with different additives.<sup>10,12-14</sup> Despite all this effort, any of them has challenged the cyanide bath plating system.

Among the Cu-Zn alloy family, those containing up to 42 wt% of zinc are the most important for technical applications. In this composition range, the alloy consists only of  $\alpha$ -brass up to 32 wt% of zinc according to the Cu-Zn equilibrium diagram (Figure 1). This phase presents higher ductility than pure copper and is less expensive. Moreover, brass coatings are particularly used to favor adhesion of rubber to steel. For example, the steel meshes that reinforce radial tires are electrolytically covered with Cu-Zn alloys containing between 30 and 37 wt% of zinc<sup>15,16</sup> to prevent occurrence of blisters in the tires.

Amino acids are known to form stable complexes with some metallic ions,<sup>17</sup> particularly in mildalkaline media. In a previous work,<sup>18</sup> glutamic acid was used as an effective complexing agent to replace cyanide in copper plating baths. Glutamate ion (Glu) was chosen mainly for three reasons: 1) it forms a stable negatively-charged complex with Cu<sup>2+</sup> ([CuGlu<sub>2</sub>]<sup>2-</sup>) as cyanide does with Cu<sup>+</sup>; 2) it is used in the food industry as flavor enhancer and is not dangerous to human health; 3) it is available at an affordable price in the market.

The Glu-based copper electrolyte reduces the harmful effects of cyanide and replaces the copper strike process since it allows working at pH values in which substrates, such as steel, or zinc do not corrode.<sup>19,20</sup> Glu ion has been also used as complexing agent to obtain zinc electrodeposits on steel with excellent adherence, brightness and quality performance.<sup>21</sup> Based on these results, Glu seems a good candidate for brass electrodeposition.

The aim of the present study was to carry out a preliminary study to evaluate a Glu-containing electrolyte as candidate to obtain Cu-Zn alloy coatings, determining the electrolyte composition and current

density ranges in which compositions of nearly 30 wt% of Zn can be obtained.

## Materials and Methods

Table I shows the concentrations of Cu<sup>2+</sup> (CuSO<sub>4</sub>·5H<sub>2</sub>O) and Zn<sup>2+</sup> (ZnSO<sub>4</sub>·7H<sub>2</sub>O) used in the electrolytes under study. In all the cases concentration of the complexing agent (C<sub>5</sub>H<sub>8</sub>NO<sub>4</sub>Na) was 0.6 M and the pH was adjusted to a value of 9 using KOH. The solutions C and Z were prepared with a 0.6 M concentration of Glu and pH = 9 to compare the electrochemical behavior of each cation with that of the mixed electrolytes.

The 267 ml- Hull cell (Kocour Co.) with thermostat and air agitation was used to obtain deposits in a wide range of current density (j). For all the cases, temperature was set at 60±1°C. The steel cathodes (Q-Panel SmoothFinish QD-36) were pickled in a 10% v/v H<sub>2</sub>SO<sub>4</sub> solution. The electrodeposition was conducted during 1 minute at 2 A. The composition of the coatings was determined with a scanning electron microscope (SEM) Quanta200 FEI (Tungsten filament source) equipped with an EDS detector.

Cyclic voltammeteries (CV) were conducted using a jacketed glass cell connected to a Frigomix 1495 thermostat to maintain the temperature of the electrolyte at 60°C. A standard three-electrode cell was used with a platinum disc (A = 0.041 cm<sup>2</sup>) as working electrode. A platinum wire (A = 4.70 cm<sup>2</sup>) was the counter electrode and a saturated calomel electrode (SCE) was used as reference electrode. All the potential values in this work are expressed in this scale. The essays were conducted with a PAR potentiostat/ galvanostat model 273A connected to a computer and monitored by the CorrWare2 software. Potential scanings were carried out between -1 V and 1 V for the C bath and between -1.7 V and 1 V for the rest of the electrolytes, with a scan rate of 50 mV/s. Another CV was carried out in a 0.6 M sodium glutamate solution at pH 9 using an electrode made of commercial

Table I. Electrolytes used.

Electrolyte	Cu <sup>2+</sup> (M)	Zn <sup>2+</sup> (M)	Molar % Cu <sup>2+</sup>
L <sub>90</sub>	0.20	0.02	90
L <sub>80</sub>	0.20	0.05	80
L <sub>70</sub>	0.20	0.09	70
L <sub>60</sub>	0.20	0.13	60
L <sub>40</sub>	0.13	0.2	40
L <sub>30</sub>	0.09	0.2	30
L <sub>20</sub>	0.05	0.2	20
L <sub>10</sub>	0.02	0.2	10
C	0.2	0	100
Z	0	0.2	0

<sup>z</sup>E-mail: p.pary@cidepint.gov.ar

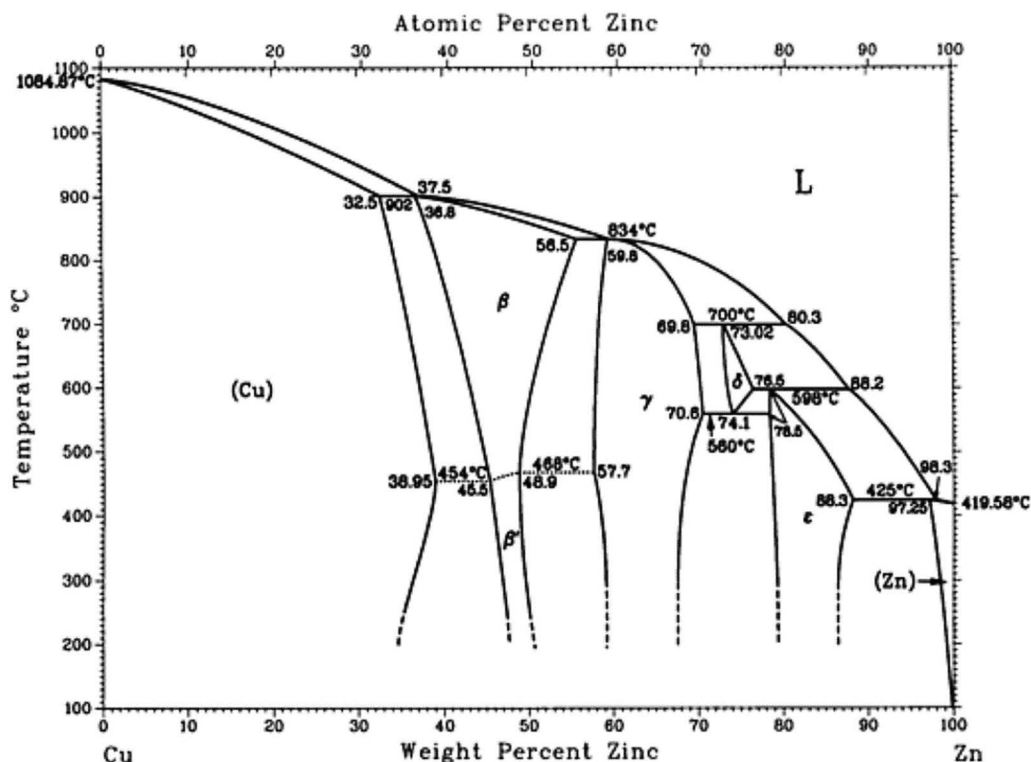


Figure 1. Cu-Zn phase diagram (ASTM Metals Handbook Volume 3).

Cu-Zn/70–30 alloy in order to compare the observed behavior with the commercial brass anodic dissolution.

Deposits on flat steel electrodes of 6 cm<sup>2</sup> surface area were obtained. The electrodes were also pickled in a 10% v/v H<sub>2</sub>SO<sub>4</sub> solution. Afterwards, the deposition was carried out in a glass cell at 60±1°C and magnetic agitation. The anode was of the same size as the cathodes and made out of Cu-Zn/70–30 commercial alloy. In all cases, time was set to obtain a theoretical coating thickness of 5 μm considering pure copper in Faraday's Law.

## Results and Discussion

**Hull cell.**—In the Hull cell, current density on the cathode varies according to Equation 1.<sup>22</sup>

$$j(x) = j_{avg} \left[ 2.33 * \log \left( \frac{1}{1-x} \right) - 0.08 \right] \quad [1]$$

$$x = h/L$$

$j(x)$  is the local current density,  $j_{avg}$  is the average current density on the cathode calculated as the total applied current ( $I$ ) divided by the cathode area,  $h$  is the distance from the cathode edge and  $L$  is the total length of the cathode. For this study, six different  $j(x)$  were selected, from  $j_1 = 0.001$  to  $j_6 = 0.086$  A/cm<sup>2</sup> so that a simple screening test could be done.

The composition of the coatings obtained by SEM/EDS at each  $j(x)$  vs the composition of the electrolyte is presented in Figure 2. In almost all the cases, the molar % of Cu in the alloy ( $X_{Cu}$ ) is equal or higher than the molar % Cu<sup>2+</sup> in the electrolyte ( $X_{Cu^{2+}}$ ). This behavior was different ( $X_{Cu} < X_{Cu^{2+}}$ ) for baths L<sub>30</sub> and L<sub>40</sub> when  $j(x) \geq j_4$ , though the deviation was not significant. These results show that electrolytes with higher concentrations of Cu<sup>2+</sup> favor the deposition of alloys with higher percentage of Cu. Regarding the effect of  $j$ , for the same electrolyte the amount of copper in the coating decreased when  $j(x)$  increases, being this effect more important for lower  $X_{Cu^{2+}}$ . The data corresponding to the deposits obtained with baths with  $X_{Cu^{2+}} >$

50% showed  $X_{Cu} > 70\%$  for all  $j(x)$ , whereas coatings deposited using electrolytes with  $X_{Cu^{2+}} < 50\%$  had varied compositions with  $10\% < X_{Cu} < 90\%$  depending on  $j(x)$ . There is an anomalous behavior at  $j \leq j_3$  since the  $X_{Cu}$  is higher for bath L10 than it is for L20 and L30 and this effect could deserve further investigation although this extremely low  $X_{Cu^{2+}}$  has no practical consideration.

Hull cell tests results suggest that the Cu-Zn-Glu electrolyte behaves as a regular system according to Brenner's classification<sup>23</sup> of alloy plating electrolytes where the most noble metal is deposited preferentially on the cathode.

These regular systems are usually characterized by being under diffusional control. It is widely known that noble metals reach their limiting current density at more anodic potentials than the active

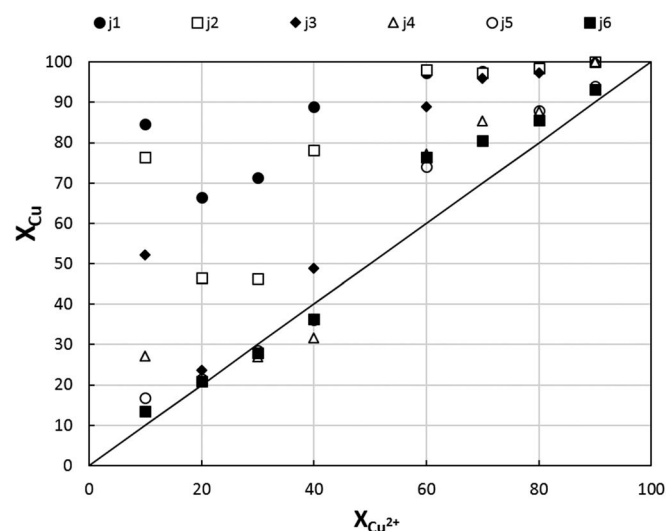
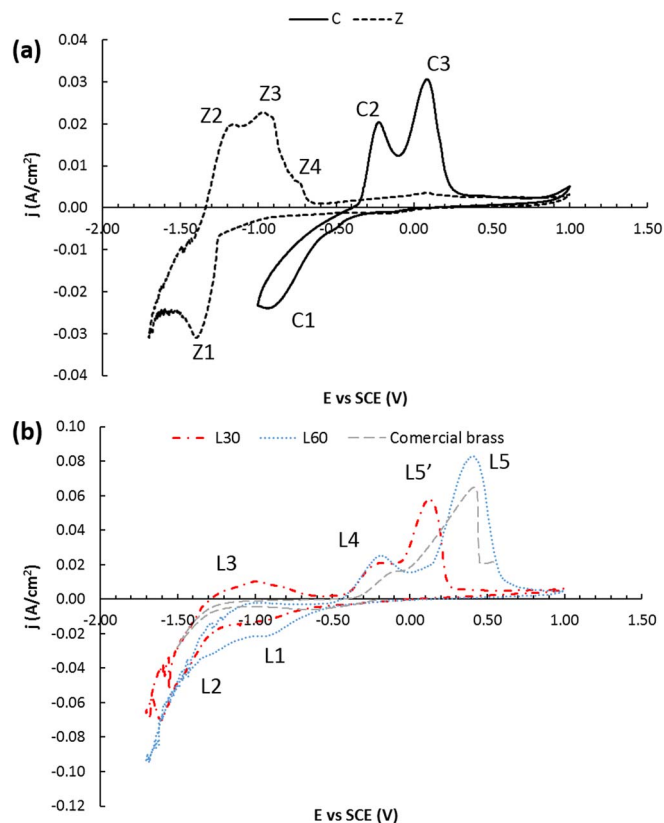


Figure 2.  $X_{Cu}$  in the deposit vs.  $X_{Cu^{2+}}$  in the electrolyte for selected  $j$  values.



**Figure 3.** CV recorded at 50 mV/s for (a) C and Z electrolytes, (b) L60 and L30 and commercial brass.

metals. Consequently, working at higher  $j$  (larger polarization) would increase the amount of zinc in the coating since the deposition of copper would be already limited by mass transport. At low  $j$ , the deposits were majorly formed by copper; when  $j$  increased, the  $X_{\text{Cu}}$  decreased, reaching almost a constant value close to the  $X_{\text{Cu}}^{2+}$  in the electrolyte. Moreover, as the system is under mass-transfer control, all the variables that increase the concentration of ions near the cathode will increase the  $X_{\text{Cu}}$ .

From the group of electrolytes with  $[\text{Cu}^{2+}] = 0.2 \text{ M}$ ,  $L_{60}$  was the only one that showed deposits with compositions close to commercial brass at  $j_5$ . By the other side, from the group of electrolytes with  $[\text{Zn}^{2+}] = 0.2 \text{ M}$ ,  $L_{20}$  and  $L_{30}$  at  $j_1$  produced coatings with  $X_{\text{Cu}}$  close to the objective (67% and 71%, respectively). In order to continue the electrochemical characterization, two electrolytes were selected that could be candidates for obtaining coatings with compositions similar to  $X_{\text{Cu}} = 70\%$ :  $L_{60}$  from the  $[\text{Cu}^{2+}] = 0.2 \text{ M}$  group and electrolyte  $L_{30}$  was chosen from the  $[\text{Zn}^{2+}] = 0.2 \text{ M}$  group, as the appearance of the deposits from Hull cell tests was brighter than  $L_{20}$  in the range of  $j$  of interest.

**Cyclic voltammetry.**—The electrochemical behavior of  $L_{30}$  and  $L_{60}$  electrolytes was studied by CV and was compared to that of the baths containing only  $\text{Cu}^{2+}$  or  $\text{Zn}^{2+}$ .

Figure 3a shows the voltamperometric results obtained for C and Z electrolytes. The curve for C presents only one cathodic peak (C1) at  $-0.9 \text{ V}$ , usually assigned to the reduction of the cupric ion to metallic copper.<sup>11,24,25</sup> This reaction occurs in a two-stage mechanism with a  $\text{Cu}^+$  soluble complex ( $\text{Cu}^{+*}$ ) as intermediate species.<sup>18,26,27</sup> Two anodic peaks were observed; C2 was at  $-0.25 \text{ V}$  and C3 at  $0.10 \text{ V}$ . These peaks were assigned to the oxidation of the absorbed  $\text{Cu}^{+*}$  and to the oxidation of metallic copper, respectively.<sup>18</sup>

In the CV for the Z electrolyte, a cathodic peak (Z1) is observed at  $-1.4 \text{ V}$ . This peak has been reported by other authors for similar potentials and attributed to the reduction of  $\text{Zn}^{2+}$ .<sup>28,29</sup> Also, three an-

odic peaks were registered: Z2 at  $-1.2 \text{ V}$ , Z3 at  $-0.96 \text{ V}$  and Z4 at  $-0.73 \text{ V}$ . Z2 can be assigned to the dissolution of the metallic Zn as has been reported in alkaline media.<sup>29–32</sup> Although the composition of electrolytes used by other authors are in general concentrated NaOH, the potential of Z3 agrees fairly well with that reported for the precipitation of  $\text{Zn}(\text{OH})_2$  in the first stage of the oxidation process.<sup>28,30,33</sup> The passivation of the Zn surface is given by the formation of a ZnO film at  $-0.86 \text{ V}$  in NaOH solutions, though for the Z electrolyte, this potential (Z4) is displaced toward more anodic values probably due to the lower pH and the presence of the Glu ion. It is important at this point to recall that the dissociation constant of the zinc glutamate complex is in the order of  $10^{-9}$  and consequently can compete with hydroxide and oxide formation.

It is important to notice the polarization of the copper and zinc reduction reactions to more cathodic overpotentials values due to the complexation with Glu. The presence of the complexing agent moves from  $0.1 \text{ V}$  ( $\text{Cu}^{2+}$  standard reduction potential) to  $-0.9 \text{ V}$  the deposition potential for copper and from  $-1.0 \text{ V}$  ( $\text{Zn}^{2+}$  standard reduction potential) to  $-1.4 \text{ V}$  for zinc. For that reason, the simultaneous reduction of copper and zinc in the same electrolyte can be studied in a wide potential window ( $-0.5 \text{ V}$  to  $-1.5 \text{ V/SCE}$ ).

CVs obtained with  $L_{60}$  and  $L_{30}$  showed a different behavior with respect to C and Z electrolytes. In the CV for  $L_{60}$  (Figure 3b), the peak L1 is at the same potential as C1, suggesting its correspondence to the  $\text{Cu}^{2+}$  reduction. However, peak L2 does not seem to be assignable to zinc deposition because it appears at  $-1.3 \text{ V}$ , showing an anodic shift (150 mV) with respect to Z1. This could indicate that a Cu-Zn alloy is being deposited at that potential.<sup>34–36</sup> The current densities of both peaks (L1 and L2) are of the same order than C1 and Z1. During the scanning in the anodic direction, no comparable peaks to Z2, Z3 or Z4 are defined, indicating that anodic dissolution of Zn is inhibited. Conversely, the peak L4 is clearly defined in the same position as C2 in Figure 3a. It may correspond to the oxidation process of the intermediate  $\text{Cu}^{+*}$ . Finally, the peak L5 is defined at a more anodic potential, with no agreement with the location of C3 in Figure 3a. Consequently, the anodic dissolution process responsible for L5 is not considered as the dissolution of the metallic copper. The CV carried out in a 0.6 M sodium glutamate solution at pH 9 using an electrode made of commercial Cu-Zn/70–30 alloy is presented in Figure 3b). The potential of the anodic peak is  $0.4 \text{ V}$  as well as for L5. Therefore, for these conditions, there seem to be a co-deposition of both metals forming an alloy with a similar electrochemical behavior as commercial brass.

In the cathodic scanning for the  $L_{30}$  bath the peak L1 is also observed, though its peak current density ( $j_p = 0.01 \text{ A/cm}^2$ ) is 50% lower than the  $j_p$  ( $0.02 \text{ A/cm}^2$ ) registered for peak L1 using  $L_{60}$ . This fact can be explained due to the lower concentration of the cupric ion since  $j_p$  is a linear function of the metallic ion concentration in both reversible and irreversible electrochemical processes.<sup>37</sup> During the anodic swept, a low anodic current density was detected for electrochemical potentials between  $-1.4 \text{ V}$  and  $-0.6 \text{ V}$  (L3), values where the anodic dissolution of metallic Zn is expected. This fact indicate that the amount of Zn deposited during the cathodic scanning is higher than for the case of the  $L_{60}$  electrolyte.

For more anodic potentials, L4 appears without modifications as it was expected since this process is due to the  $\text{Cu}^{+*}$  soluble intermediate.<sup>18</sup> It should be noted that the peak indicated as L5' in Figure 3b was registered at the same potential than the dissolution peak of the metallic copper (C3 in Figure 3a). This behavior is consistent with the independent anodic dissolution of the two metals for  $L_{30}$  and supports the assignment of peak L5 to the dissolution of a Cu-Zn alloy in the CV for  $L_{60}$ .

**Cu-Zn galvanostatic deposits.**—Electrolytes  $L_{30}$  and  $L_{60}$  were used to deposit Cu-Zn alloys at different  $j$ , starting from the value where the  $X_{\text{Cu}}$  was closer to 70% in Hull cell screening tests (Figure 2). The conditions in which the coatings were obtained, the EDS analysis results and the faradaic efficiency are presented in Table II. The appearance of the deposits is shown in Figure 4.

**Table II. Working conditions for flat deposits on steel electrodes and composition of the deposited alloy.**

Deposit	Electrolyte	$j$ (A/cm <sup>2</sup> )	$X_{\text{Cu}}$	Faradaic efficiency
1	L <sub>60</sub>	0.0430	100	91
2	L <sub>60</sub>	0.0861	100	100
3	L <sub>60</sub>	0.1292	87.7	93
4	L <sub>30</sub>	0.0043	97.0	75
5	L <sub>30</sub>	0.0258	81.3	100
6	L <sub>30</sub>	0.0646	51.5	100

The appearance of coating 1 was similar and almost identical to pure copper deposits obtained from copper-Glu electrolytes.<sup>18</sup> However, deposits 2 to 6 presented different colorations with some yellowish tendency. Coatings obtained at higher  $j$  for each electrolyte, samples 3 and 6 in Figure 4, show some edge effects because of the use of simple flat geometry electrodes. Coating 6 has a typical brass lustre in the center of the sample but strong edge effects. Homogeneity in coloration is a key issue in alloy electrodeposition. Further studies with better current distribution geometry are needed to improve this subject.

The composition analysis by EDS agreed with the coloration pattern described above (Table II). It is important to mention that when using L<sub>60</sub> it was necessary to reach considerably high values of

$j$  ( $\approx 0.13$  A/cm<sup>2</sup>) in order to obtain a Cu-Zn alloy instead of pure copper whereas for L<sub>30</sub>, at  $j \approx 0.07$  A/cm<sup>2</sup>  $X_{\text{Cu}}$  decreased to  $\approx 50\%$ .

The SEM images (Figure 5) showed the same smooth, slightly globular, surface morphology for all deposits. Microcracks were found in almost all the samples as it has been usually found with other non-cyanide electrolytes.<sup>5,38</sup>

## Conclusions

Formulations containing sodium glutamate as complexing agent are a suitable alternative for Cu-Zn electrodeposition and deserve deeper investigation.

The Hull cell screening tests allowed the characterization of the system under study as regular according to Brenner alloy plating classification criteria, given that the more noble metal (Cu) was deposited preferentially.

The reduction and oxidation processes studied are affected by the  $X_{\text{Cu}}^{2+}$  in the electrolyte. CV recorded with bath L<sub>30</sub> showed cathodic peaks corresponding to the deposition of Cu and a Cu-Zn alloy and two anodic peaks which matched the dissolution potentials of Zn and Cu in baths C and Z. Electrolyte L<sub>60</sub> presented the same cathodic peaks as C and Z electrolytes but only one dissolution process was registered coinciding with the anodic peak of a commercial brass in a glutamate solution at pH = 9. The complexation with Glu caused the

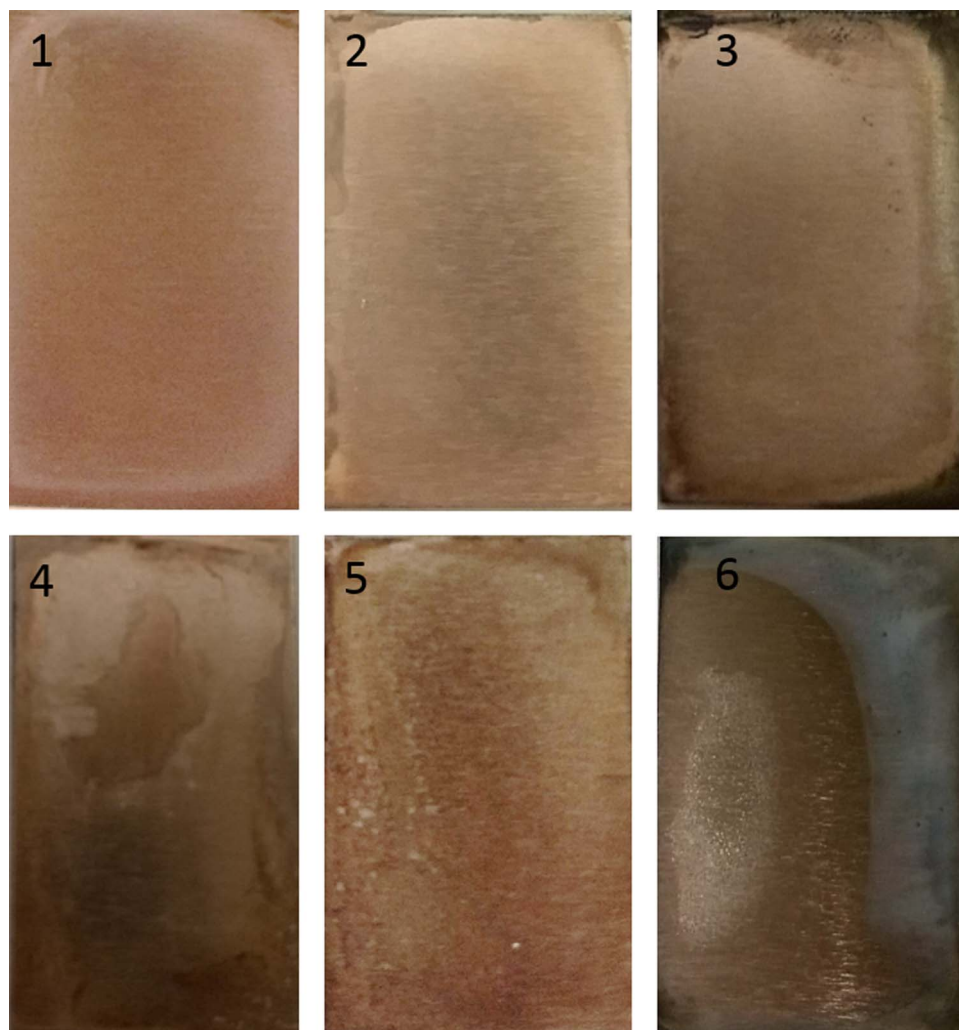


**Figure 4.** Cu-Zn deposits obtained with bath L<sub>60</sub> at (1)  $j = 0.0430$  A/cm<sup>2</sup> (2)  $j = 0.0861$  A/cm<sup>2</sup> (3)  $j = 0.1292$  A/cm<sup>2</sup> and L<sub>30</sub> (4)  $j = 0.0043$  A/cm<sup>2</sup> (5)  $j = 0.0258$  A/cm<sup>2</sup> (6)  $j = 0.0646$  A/cm<sup>2</sup>.



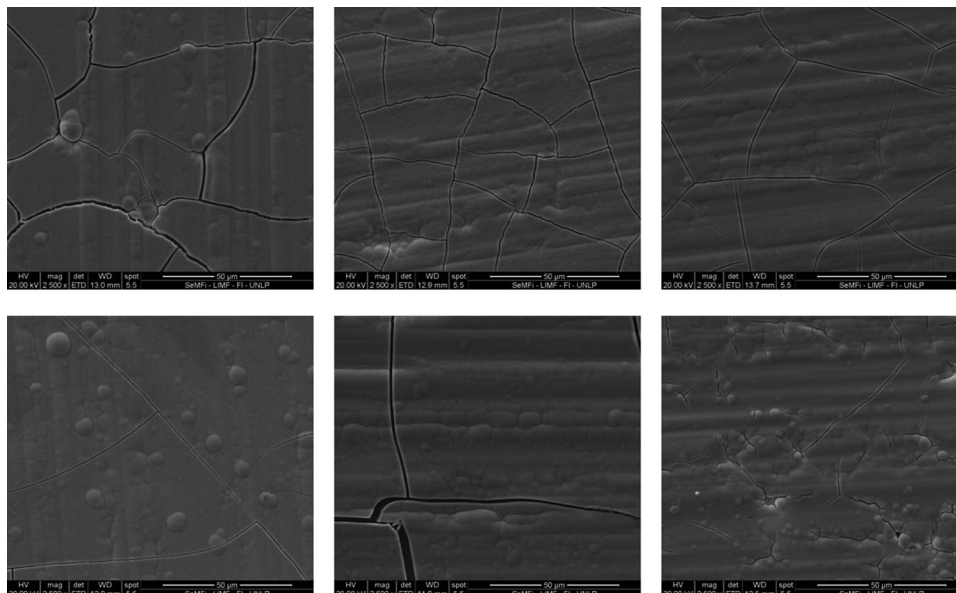


**Figure 5.** SEM images of the Cu-Zn deposits obtained with bath L<sub>60</sub> at (1) 0.0430 A/cm<sup>2</sup> (2) 0.0860 A/cm<sup>2</sup> (3) 0.1292 A/cm<sup>2</sup> and L<sub>30</sub> (4) 0.0043 A/cm<sup>2</sup> (5) 0.0258 A/cm<sup>2</sup> (6) 0.0646 A/cm<sup>2</sup>.

polarization of the copper and zinc reduction reactions favoring the codeposition of copper and zinc.

Results of the present study suggest that future research on the production and characterization of electrodeposited Cu-Zn alloys should be approached using electrolytes with compositions similar to L<sub>30</sub>.

### Acknowledgments

The authors thank the Comisión de Investigaciones Científicas de la Provincia de Buenos Aires (CICPBA), Consejo Nacional de Investigaciones Científicas y Técnicas (CONICET) and the Universidad Nacional de La Plata (UNLP) for their financial support to this research.

### ORCID

P. Pary <https://orcid.org/0000-0002-2541-9938>

L. N. Bengoa <https://orcid.org/0000-0002-0608-8248>

W. A. Egli <https://orcid.org/0000-0003-0477-660X>

### References

1. A. Brenner, in *Electrodeposition of alloys, Principles and practice*, Vol. 1, p. 411, Academic Press, New York, USA, (1963).
2. J. W. Dini and D. D. Snyder, in *Modern electroplating*, M. Schlesinger and M. Paunovic, eds., p. 33, Wiley, USA, (2010).
3. R. Winand, in *Modern electroplating*, M. Schlesinger and M. Paunovic, eds., John Wiley & sons Inc., New Jersey, (2010).
4. N. Piccinini, G. N. Ruggiero, G. Baldi, and A. Robotto, *Journal of Hazardous Materials*, **71**(1–3), 395 (2000).
5. T. Vagrameyan, J. S. L. Leach, and J. R. Moon, *Electrochimica Acta*, **24**(2), 231 (1979).
6. A. R. Despić, V. Marinović, and V. Jović, *Journal of Electroanalytical Chemistry*, **339**(1–2), 473 (1992).
7. K. Johannsen, D. Page, and S. Roy, *Electrochimica Acta*, **45**(22), 3691 (2000).
8. L. F. D. Senna, S. L. Dfaz, and L. Sathler, *Materials Research*, **8**, 275 (2005).
9. R. Krishnan, V. Muralidharan, and S. Natarajan, *Bulletin of electrochemistry*, **12**(5–6), 274 (1996).
10. M. R. H. de Almeida, E. P. Barbano, M. F. de Carvalho, P. C. Tulio, and I. A. Carlos, *Applied Surface Science*, **333**(Supplement C), 13 (2015).
11. J. C. Ballesteros, E. Chañet, P. Ozil, G. Trejo, and Y. Meas, *Journal of Electroanalytical Chemistry*, **645**(2), 94 (2010).
12. I. A. Carlos and M. R. H. de Almeida, *Journal of Electroanalytical Chemistry*, **562**(2), 153 (2004).
13. A. Survila, Z. Mockus, S. Kanapeckaitė, and G. Stalnis, *Electrochimica Acta*, **94**, 307 (2013).
14. R. Özdemir, İ. H. Karahan, and O. Karabulut, *Metallurgical and Materials Transactions A*, **47**(11), 5609 (2016).
15. W. V. Ooij, *Rubber Chemistry and Technology*, **52**(3), 605 (1979).
16. A. Maesele and E. Debruyne, *Rubber Chemistry and Technology*, **42**(2), 613 (1969).
17. R. M. Smith and A. E. Martell, in *Critical stability constants. Volumen 6-Second Supplement*, Vol. 6, Plenum Press, (1989).
18. P. Pary, L. N. Bengoa, and W. A. Egli, *Journal of The Electrochemical Society*, **162**(7), D275 (2015).
19. M. Pourbaix, in *Atlas of Electrochemical Equilibria in Aqueous Solutions*, p. 307, National Association of Corrosion Engineers, Houston, Texas, USA, (1974).
20. M. Pourbaix, in *Atlas of Electrochemical Equilibria in Aqueous Solutions*, p. 406, National Association of Corrosion Engineers, Houston, Texas, USA, (1974).
21. J. Baliño, P. Pary, L. N. Bengoa, P. R. Seré, and W. A. Egli, in “18° Congreso Internacional de Metalurgia y Materiales SAM-CONAMET 2018 <http://fisica.cab.cnea.gov.ar/sam-conamet18/listado-de-resumenes/>”, p. 871. Comisión Nacional de Energía Atómica - CNEA, Bariloche, Argentina, 2018.
22. D. R. Gabe, *Metal Finishing*, **105**(10), 511 (2007).
23. A. Brenner, *Electrodeposition of alloys, Principles and practice*, Academic Press, New York, USA (1963).
24. A. E. Bolzán, *Electrochimica Acta*, **113**, 706 (2013).
25. D. Grujicic and B. Pesic, *Electrochimica Acta*, **47**(18), 2901 (2002).
26. E. Mattsson and J. O. M. Bockris, *Transactions of the Faraday Society*, **55**, 1586 (1959).
27. D. Grujicic and B. Pesic, *Electrochimica Acta*, **50**(22), 4426 (2005).
28. M. Cai and S. M. Park, *Journal of The Electrochemical Society*, **143**(7), 2125 (1996).
29. J. L. Ortiz-Aparicio, Y. Meas, G. Trejo, R. Ortega, T. W. Chapman, and E. Chañet, *Journal of Applied Electrochemistry*, **43**(3), 289 (2013).
30. M. Cai and S. M. Park, *Journal of The Electrochemical Society*, **143**(12), 3895 (1996).
31. P. Sonneveld, W. Visscher, and E. Barendrecht, *Electrochimica acta*, **37**(7), 1199 (1992).
32. R. Powers and M. Breiter, *Journal of the Electrochemical Society*, **116**(6), 719 (1969).
33. M. C. H. McKubre and D. D. Macdonald, *Journal of The Electrochemical Society*, **128**(3), 524 (1981).
34. M. De Almeida, E. Barbano, M. De Carvalho, I. Carlos, J. Siqueira, and L. Barbosa, *Surface and Coatings Technology*, **206**(1), 95 (2011).
35. J. C. Ballesteros, L. M. Torres-Martínez, I. Juárez-Ramírez, G. Trejo, and Y. Meas, *Journal of Electroanalytical Chemistry*, **727**(Supplement C), 104 (2014).
36. M. Li, G. Wei, S. Hu, S. Xu, Y. Yang, and Q. Miao, *Surface Review and Letters*, **22**(01), 1550003 (2015).
37. A. J. Bard and L. R. Faulkner, in *Electrochemical Methods. Fundamentals and applications*, p. 231, John Wiley & Sons, INC, USA, (2001).
38. S. M. Rashwan, *Transactions of the IMF*, **85**(4), 217 (2007).